

Neutron Stars and Massive Quark Matter

A. Drago and U. Tambini

Dipartimento di Fisica, Università di Ferrara, and INFN, Sezione di Ferrara, Via Paradiso 12, I-44100 Ferrara, Italy

M. Hjorth-Jensen

ECT, European Centre for Theoretical Studies in Nuclear Physics and Related Areas, Trento, Italy*

Using the Color-Dielectric model to describe quark confinement, including strange quarks and accounting for beta-equilibrium, we get masses for a static neutron star in the range $1.3 \leq M/M_\odot \leq 1.54$ for a radius $R \approx 9$ km. Rapid cooling through the direct URCA mechanism is obtained. The implications for the composition of neutron stars is discussed.

PACS numbers: 97.60.Jd, 12.39.-x, 24.85.+p

The equation of state (EOS) for dense matter is central to calculations of neutron-star properties, such as the mass range, the mass-radius relationship, the crust thickness and the cooling rate, see e.g. Refs. [1–3]. The same EOS is also crucial in calculating the energy released in a supernova explosion.

The typical density range of a neutron star stretches from central densities of the order of 5 to 10 times the nuclear matter saturation density $n_0 = 0.17 \text{ fm}^{-3}$ to zero at the edge of the star. Clearly, the relevant degrees of freedom will not be the same in the crust, where the density is much smaller than n_0 , and in the center of the star where the density is so high that models based solely on interacting nucleons are questionable. Data from neutron stars indicate that the EOS should probably be moderately stiff in order to support maximum neutron star masses in a range from approximately $1.4M_\odot$ to $1.9M_\odot$ [4]. In addition, simulations of supernovae explosions seem to require an EOS which is even softer. A combined analysis of the data coming from binary pulsar systems and from neutron star formation scenarios can be found in Ref. [5], where it is shown that neutron star masses should fall predominantly in the range $1.3 \leq M/M_\odot \leq 1.6$.

Several theoretical approaches to calculations of the EOS have been considered. The hypothesis that strange quark matter may be the absolute ground state of the strong interaction [6], has been used by several authors in the investigation of the possibility of interpreting pulsars as rotating strange stars [7,8]. Other approaches introduce exotic states of nuclear matter, such as kaon [9–12] or pion condensation [13,14].

The scope of this work is to study properties of neutron stars like cooling rate, total mass and radius employing a massive quark model, the so-called Color-Dielectric model (CDM) [15–17]. A very important feature of matter, as described using the CDM model, is that the deconfinement phase transition happens at a density of the order of 2–3 times n_0 , a density expected to be reached in the interior of a neutron star. Neutron stars, when studied using the CDM, consist of an exterior region described, *e.g.*, by the equation of state of Friedman and Pandharipande [18], and an interior region of quark matter. Moreover, the effective quark mass in the CDM is always larger than a value of the order of 100 MeV, hence chiral symmetry is broken and the Goldstone bosons are relevant degrees of freedom. This is to be contrasted with models like the MIT bag, where quarks have masses of a few MeV. We therefore expect the CDM to be relevant for computing the cooling rate of neutron stars *via* the URCA mechanism, as suggested by Iwamoto [19].

The CDM is a confinement model which has been used with success to study properties of single nucleons, such as structure functions [20] and form factors [21], or to describe the interaction potential between two nucleons [22], or to investigate quark matter [17,23]. In particular, it is possible, using the same set of parameters, both to describe the single nucleon properties and to obtain meaningful results for the deconfinement phase transition [17]. The aim here is therefore to see whether this model gives reasonable predictions for neutron star observables.

The Lagrangian¹ of the model is given by:

$$\begin{aligned} \mathcal{L} = & i\bar{\psi}\gamma^\mu\partial_\mu\psi \\ & + \sum_{f=u,d} \frac{g_f}{f_\pi\chi} \bar{\psi}_f (\sigma + i\gamma_5\vec{\tau}\cdot\vec{\pi}) \psi_f + \frac{g_s}{\chi} \bar{\psi}_s\psi_s \\ & + \frac{1}{2}(\partial_\mu\chi)^2 - V(\chi) \end{aligned} \quad (1)$$

¹ Throughout this paper we set $G = c = \hbar = 1$, where G is the gravitational constant.

$$+ \frac{1}{2}(\partial_\mu \sigma)^2 + \frac{1}{2}(\partial_\mu \vec{\pi})^2 - U(\sigma, \vec{\pi}),$$

where $U(\sigma, \vec{\pi})$ is the ‘‘mexican-hat’’ potential, as in Ref. [24]. The lagrangian \mathcal{L} describes a system of interacting u , d and s quarks, pions, sigmas and a scalar–isoscalar chiral singlet field χ whose potential $U(\chi)$ is given by

$$V(\chi) = \frac{1}{2}\mathcal{M}^2\chi^2. \quad (2)$$

The coupling constants are given by $g_{u,d} = g(f_\pi \pm \xi_3)$ and $g_s = g(2f_K - f_\pi)$, where $f_\pi = 93$ MeV and $f_K = 113$ MeV are the pion and the kaon decay constants, respectively, and $\xi_3 = f_{K^\pm} - f_{K^0} = -0.75$ MeV. These coupling constants depend only on a single parameter g . This parameter is fixed, together with the mass \mathcal{M} of the χ field so as to reproduce experimental nucleon mass and radius. The $SU(3)_f$ version of the model has been introduced by Birse and McGovern [25,26].

When considering a single hadron, confinement is obtained *via* the effective quark masses $m_{u,d} = g_{u,d}\bar{\sigma}/(\bar{\chi}f_\pi)$ and $m_s = g_s/\bar{\chi}$, which diverge outside the nucleon. Indeed, the classical fields $\bar{\chi}$ and $\bar{\sigma}$ are solutions of the Euler–Lagrange equations and $\bar{\chi}$ goes asymptotically to zero at large distances.

The model parameters g and \mathcal{M} are fixed to reproduce single nucleon properties. In order to describe the single nucleon state, a double projection on linear and angular momentum eigenstates has to be performed, see Ref. [24]. We will use the parameters $g = 0.023$ GeV and $\mathcal{M} = 1.7$ GeV, giving a nucleon isoscalar radius of 0.80 fm (exp.val.=0.79 fm) and an average delta–nucleon mass of 1.129 GeV (exp.val.=1.085 GeV). A similar set of parameters has been used to compute structure functions [20] and form factors [21].

The quark matter (QM) phase is characterized by a constant value of the scalar fields and by using plane waves to describe the quarks. The total energy of QM in the mean field approximation reads

$$E_{QM} = 6V \sum_{f=u,d,s} \int \frac{d\mathbf{k}}{(2\pi)^3} \sqrt{\mathbf{k}^2 + m_f^2} \theta(k_F^f - k) + VU(\bar{\chi}) + VW(\bar{\sigma}, \vec{\pi} = 0), \quad (3)$$

where k_F^f is the Fermi momentum of quarks with flavour f .

The high–density matter in the interior of neutron stars is described by requiring the system to be globally neutral

$$(2/3)n_u - (1/3)n_d - (1/3)n_s - n_e = 0, \quad (4)$$

where $n_{u,d,s,e}$ are the densities of the u , d and s quarks and of the electrons, respectively. Moreover, the system must be in β –equilibrium, i.e. the chemical potentials have to satisfy the following equations:

$$\mu_d = \mu_u + \mu_e, \quad (5)$$

$$\mu_s = \mu_u + \mu_e. \quad (6)$$

Eqs. (4)–(6) have to be solved self–consistently together with field equations, at a fixed baryon density $n = n_u + n_d + n_s$.

In the upper part of Fig. 1, the resulting quark masses are shown as function of density. As can be seen, the quark masses are large and of the order of 100 MeV up to densities about 10 times n_0 . In the lower part of Fig. 1, the Fermi momenta of the quarks are shown. In the relevant region for neutron stars the momenta are of the order of 400 MeV. Strange quarks appear at a density of $\simeq 1/3n_0$.

The energy of the QM, as described by the CDM, is larger than the energy of nuclear matter for densities smaller than 2–3 times n_0 . For lower densities we take the results from Friedman and Pandharipande [18], listed in Table 5 of Ref. [1]. We obtain an EOS valid at all densities by joining the EOS of [18] and the CDM EOS through a Maxwell construction. The latter starts at a density $\simeq 0.1\text{fm}^{-3}$ and terminates at a density $\simeq 0.26\text{fm}^{-3}$. The energy per baryon E/A in beta–stable nuclear matter is displayed in the upper part of Fig. 2 as function of density n . In the lower part of Fig 2 we show the above Maxwell construction. For the sake of comparison we also include the results from pure neutron matter obtained with the so–called Walecka model [27] and the energy per particle obtained from a relativistic Dirac–Brueckner–Hartree–Fock (DBHF) calculation in neutron matter [28], using modern meson-exchange potential models [29]. As can be seen from Fig. 2, our CDM EOS is much softer than those obtained with either the Walecka model or the DBHF calculation.

From the general theory of relativity, the structure of a static neutron star is determined through the Tolman–Oppenheimer–Volkov equation, i.e.

$$\frac{dP}{dr} = -\frac{\{\rho(r) + P(r)\} \{M(r) + 4\pi r^3 P(r)\}}{r^2 - 2rM(r)}, \quad (7)$$

where $P(r)$ is the pressure and $M(r)$ is the gravitational mass inside a radius r . The pressure is related to the energy per particle $\mathcal{E} = E/A$ by the relation $P(n) = n^2 (\partial\mathcal{E}/\partial n)$.

The resulting mass is shown in Fig. 3, while the total mass as function of radius is displayed in Fig. 4. With the CDM we obtain a maximum mass $M_{\text{max}} \approx 1.54M_{\odot}$ and a radius of 9 km at a central density corresponding to approximately 9 times nuclear matter saturation density, in good agreement with the experimental values for the mass [4,5] and the estimate for the radius [30]. Concerning the minimum mass, we obtain a value equal to $1.3M_{\odot}$. It is also possible to compute the minimum period of rotation of the star, given by $P_m \sim (0.8\text{ms})R_{10}^{3/2}(M_{\odot}/M)^{1/2}$, where R_{10} is the radius in units of 10 km [31]. In our model we get $P_m = 0.55$ ms.

Finally, we study the neutrino and antineutrino emission, which can be responsible for rapid cooling of neutron stars (URCA mechanism). In the interior of the star, where, in our model, strange quark matter is present, the relevant reactions are:

$$d \rightarrow u + e^{-} + \bar{\nu}_e, \quad (8)$$

$$e^{-} + u \rightarrow d + \nu_e, \quad (9)$$

$$s \rightarrow u + e^{-} + \bar{\nu}_e, \quad (10)$$

$$e^{-} + u \rightarrow s + \nu_e. \quad (11)$$

To conserve momentum in the reactions, the following inequalities have to be satisfied:

$$|k_F^u - k_F^e| \leq k_F^d \leq k_F^u + k_F^e, \quad (12)$$

$$|k_F^u - k_F^e| \leq k_F^s \leq k_F^u + k_F^e. \quad (13)$$

For densities larger than 0.53 fm^{-3} , conditions (12) are satisfied and the direct URCA mechanism involving only u and d quarks can start. Conditions (13) are satisfied only for densities larger than 1.4 fm^{-3} . The URCA mechanism involving strange quarks is suppressed by a factor $\sin^2 \theta_c \simeq 0.05$ with respect to the previous process, where θ_c is the Cabibbo angle.

We compute the neutrino and antineutrino luminosity, using the ultrarelativistic expansion for the chemical potentials [19]. This approximation is reasonable because the ratio m_q/k_F is approximately equal to 0.25. One gets for the total luminosity [19]

$$\epsilon = \frac{457}{1680} G_F^2 \cos^2 \theta_c m_d^2 f k_F^u (k_B T)^6, \quad (14)$$

where $f = 1 - (m_u/m_d)^2 (k_F^d/k_F^u) - (m_e/m_d)^2 (k_F^d/k_F^e)$. To obtain the characteristic cooling time we equate the energy loss per unit volume to the rate of change of thermal energy per unit volume $\tau = c_V T/\epsilon$. Here the heat capacity of the QM is $c_V = \sum_{f=u,d,s} m_f k_F^f k_B^2 T$. We get $\tau = C \text{ 1day}/T_9^4$, where T_9 is the temperature measured in units of $10^9 \text{ }^\circ\text{K}$ and C is a constant ranging from 0.5 to ~ 10 going from heavy to light neutron stars. To compare with experiment, one should also account for possible reheating mechanisms. There are however indications [32] that temperatures of young ($\sim 10^4$ years old) neutron stars lie below that obtained through the indirect URCA processes. This suggests that cooling through exotic mechanisms, as accounted for in our model, may be a meaningful explanation. Moreover, a recent reappraisal of neutrino-pair bremsstrahlung by Pethick and Thorsson [33] indicates that this process is much less important for the thermal evolution of neutron stars than suggested by earlier calculations. In addition, since the results of Ref. [1,2] indicate that the crust of the neutron star is considerably smaller than previously estimated, and the results of Ref. [34] show that proton superconductivity in the stellar interior is substantial, thereby inhibiting the traditional URCA mechanisms, there is a possibility that exotic states of matter like QM provide a viable explanation for various properties of neutron stars.

In summary, here we show that the CDM, which has been successful in describing various properties of hadrons, also gives reasonable results for neutron star observables like the mass and radius. Further, our results for the cooling of the star, combined with the results of Refs. [1,2,33,34], may suggest that the core of the neutron star can be described by a QM phase. Lastly, supernovae simulations require an EOS which is soft [35], like ours.

This work has been supported by the Istituto Nazionale di Fisica Nucleare (INFN), Italy, the Istituto Trentino di Cultura, Trento, Italy, and the Research Council of Norway. We are also indebted to Profs. Luca Caneschi, D. Mukhopadhyay and Erlend Østgaard for critically reviewing the manuscript.

[1] C. J. Pethick, D. G. Ravenhall and C. P. Lorenz, Nucl. Phys. **A584**, 675 (1995).

- [2] C. P. Lorenz, D. G. Ravenhall and C. J. Pethick, Phys. Rev. Lett. **70**, 379 (1993).
- [3] F. Weber and N. K. Glendenning, “Hadronic Matter and Rotating Relativistic Neutron Stars”, in Proceedings of the Nankai Summer School on Astrophysics and Neutrino physics, (World Scientific, Singapore, 1993), p. 64-183.
- [4] S. E. Thorsett, Z. Arzoumanian, M. M. McKinnon and J. H. Taylor, Astrophys. J. **405**, L29 (1993).
- [5] L. S. Finn, Phys. Rev. Lett. **73**, 1878 (1994).
- [6] E. Witten, Phys. Rev. **D 30**, 272 (1984).
- [7] N. K. Glendenning, in Proceedings of the International Summer School on “Structure of Hadrons and Hadronic Matter”, (World Scientific, Singapore, 1991), 275.
- [8] A. Rosenhauer, E. F. Staubo, L. P. Csernai, T. Øvergård and E. Østgaard, Nucl. Phys. **A540**, 630 (1992).
- [9] G. E. Brown, in proceedings of Perspectives in Nuclear Structure, Niels Bohr Institute, June 14-19, 1993, Nucl. Phys. **A574**, 217c (1994).
- [10] V. Thorsson, M. Prakash and J. M. Lattimer, Nucl. Phys. **A572**, 693 (1994).
- [11] G. E. Brown, C.-H. Lee, M. Rho and V. Thorsson, Nucl. Phys. **A567**, 937 (1994).
- [12] T. Muto, R. Tamagaki and T. Tatsumi, Prog. Theor. Phys. Suppl. **112**, 159 (1993); T. Muto, T. Takatsuka, R. Tamagaki and T. Tatsumi, Prog. Theor. Phys. Suppl. **112**, 221 (1993).
- [13] A. B. Migdal, E. E. Saperstein, M. A. Troitsky and D. N. Voskresensky, Phys. Rep. **192**, 179 (1990).
- [14] T. Takatsuka, R. Tamagaki and T. Tatsumi, Prog. Theor. Phys. Suppl. **112**, 67 (1993).
- [15] H. J. Pirner, Prog. Part. Nucl. Phys. **29**, 33 (1992).
- [16] M. C. Birse, Prog. Part. Nucl. Phys. **25**, 1 (1990).
- [17] A. Drago, A. Fiolhais and U. Tambini, Nucl. Phys. **A**, in press.
- [18] B. Friedman and V. R. Pandharipande, Nucl. Phys. **A361**, 502 (1981).
- [19] N. Iwamoto, Ann. Phys. **141**, 1 (1982).
- [20] V. Barone and A. Drago, Nucl. Phys. **A552**, 479 (1993); **A560**, 1076 (1993); V. Barone, A. Drago and M. Fiolhais, Phys. Lett. **B338**, 433 (1994).
- [21] M. Fiolhais, T. Neuber and K. Goeke, Nucl. Phys. **A570**, 782 (1994); A. Drago, M. Fiolhais, U. Tambini, in preparation.
- [22] K. Bräuer, A. Drago and A. Faessler, Nucl. Phys. **A511**, 558 (1990).
- [23] W. Broniowski, M. Čibej, M. Kutschera and M. Rosina, Phys. Rev. D **41**, 285 (1990).
- [24] T. Neuber, M. Fiolhais, K. Goeke and J. N. Urbano, Nucl. Phys. **A560**, 909 (1993).
- [25] J. A. McGovern and M. C. Birse, Nucl. Phys. **A506**, 367 (1990); **A506**, 392 (1990).
- [26] J. A. McGovern, Nucl. Phys. **A533**, 553 (1991).
- [27] B. D. Serot and J. D. Walecka, Adv. Nucl. Phys. **16**, 1 (1986).
- [28] L. Engvik, M. Hjorth-Jensen, E. Osnes, G. Bao and E. Østgaard, Phys. Rev. Lett. **73**, 2650 (1994).
- [29] R. Machleidt, Adv. Nucl. Phys. **19**, 189 (1989).
- [30] R. Mittet and E. Østgaard, Phys. Rev. C **37**, 1711 (1988).
- [31] P. Haensel and J. L. Zdunik, Nature **340**, 617 (1989).
- [32] H. Umeda, N. Shibazaki, K. Nomoto and S. Tsuruta, Astr. Journ. **408**, 186 (1993).
- [33] C. J. Pethick and V. Thorsson, Phys. Rev. Lett. **72**, 1964 (1994).
- [34] F. V. De Blasio, Ø. Elgarøy, L. Engvik, M. Hjorth-Jensen, G. Lazzari and E. Osnes, in preparation.
- [35] H. A. Bethe, Rev. Mod. Phys. **62**, 801 (1990).

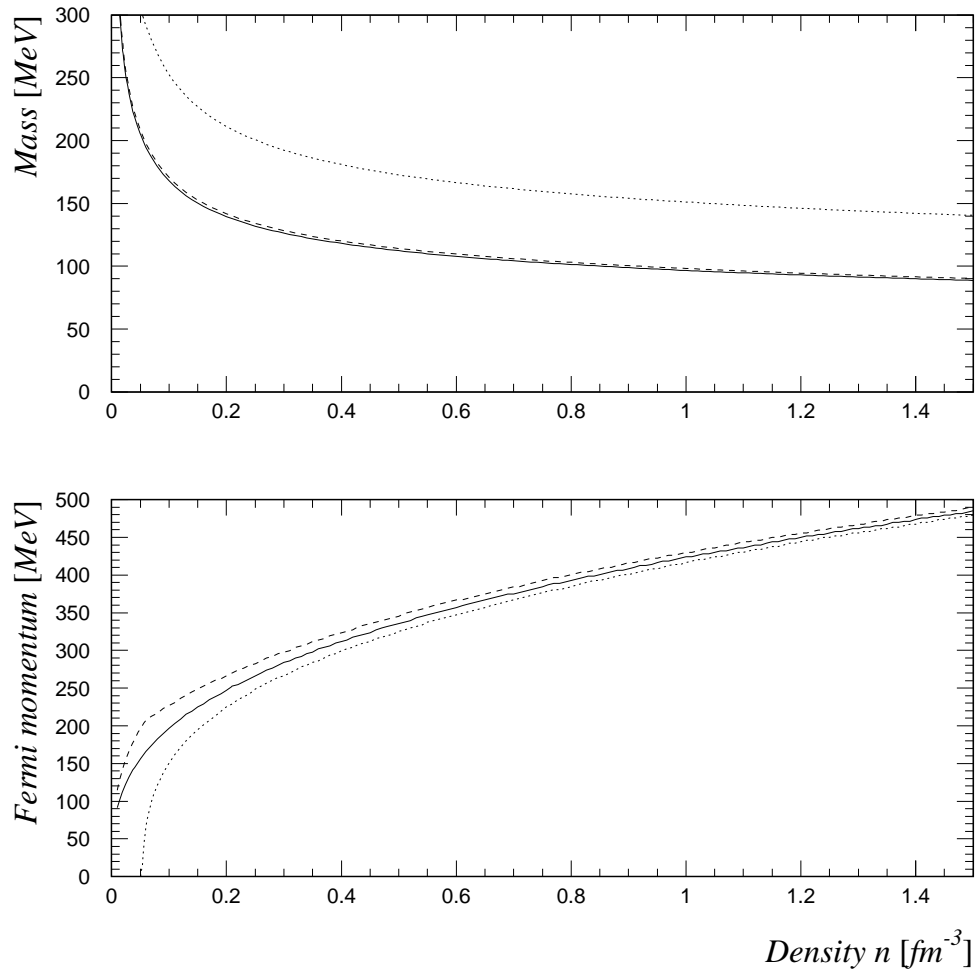


FIG. 1. The upper part shows quark masses as function of density n . In the lower figure we give the quark composition as function of density n . In both figures, solid lines are the results for u quarks, dashed lines correspond to d quarks and dotted lines are the results for s quarks.

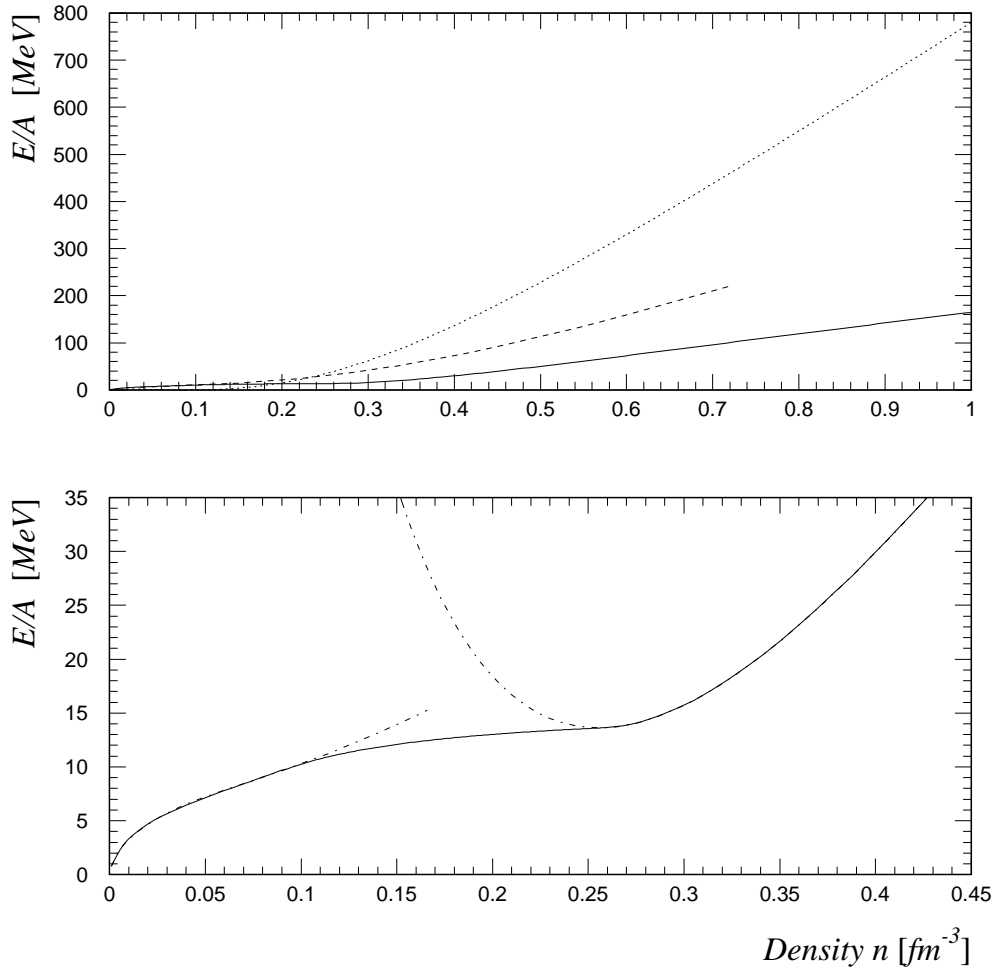


FIG. 2. The upper part gives the energy per baryon E/A as function of the density n for the three equations of state discussed in the text. The solid line corresponds to the result obtained with the CDM, the dotted line represents the result for the Walecka model, while the dashed line is the result from the DBHF calculations of Ref. [28]. In the lower figure, we show the Maxwell construction discussed in the text. The solid line is the final EOS after the Maxwell construction, the dash-dotted lines to the left (low densities) is the EOS of Ref. [18], while the dash-dotted line to the right is the CDM EOS.

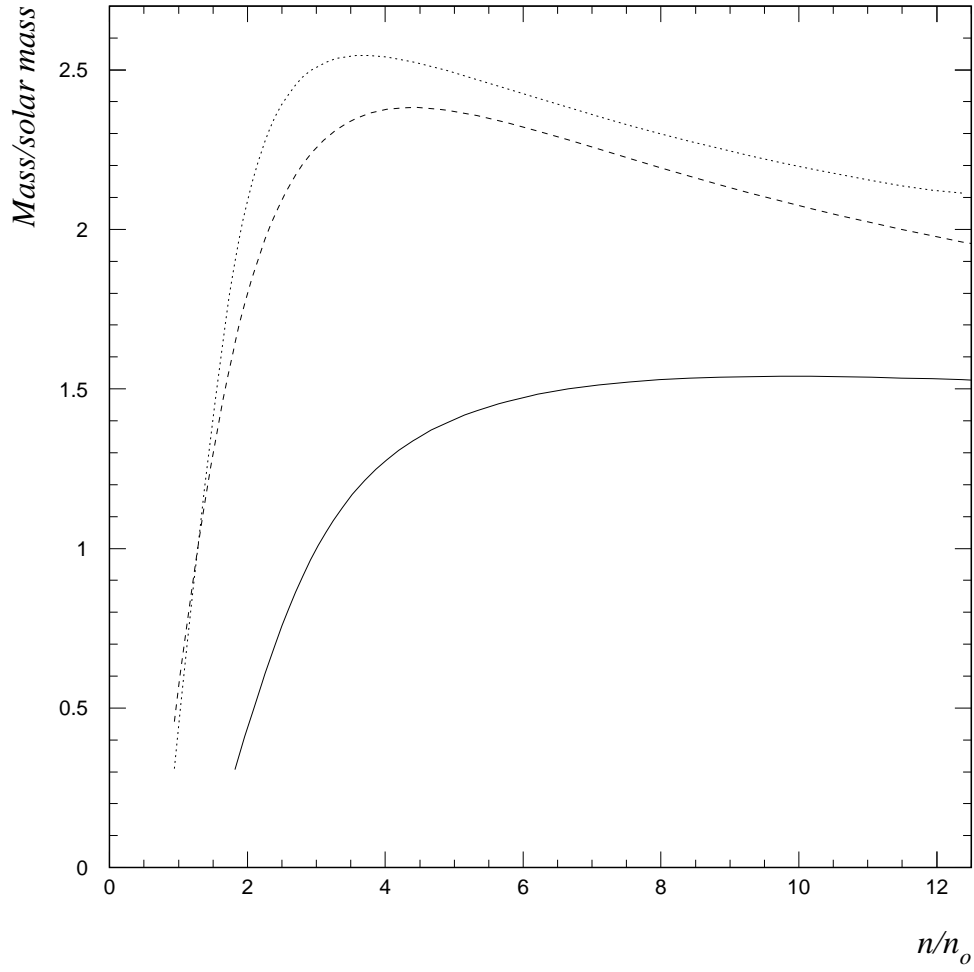


FIG. 3. M/M_{\odot} as function of n/n_0 , where n_0 is the nuclear matter saturation density $n_0 = 0.17 \text{ fm}^{-3}$. The solid line corresponds to results obtained with the CDM, the dotted line represents results for the Walecka model, while the dashed line are results from the DBHF calculations of Ref. [28].

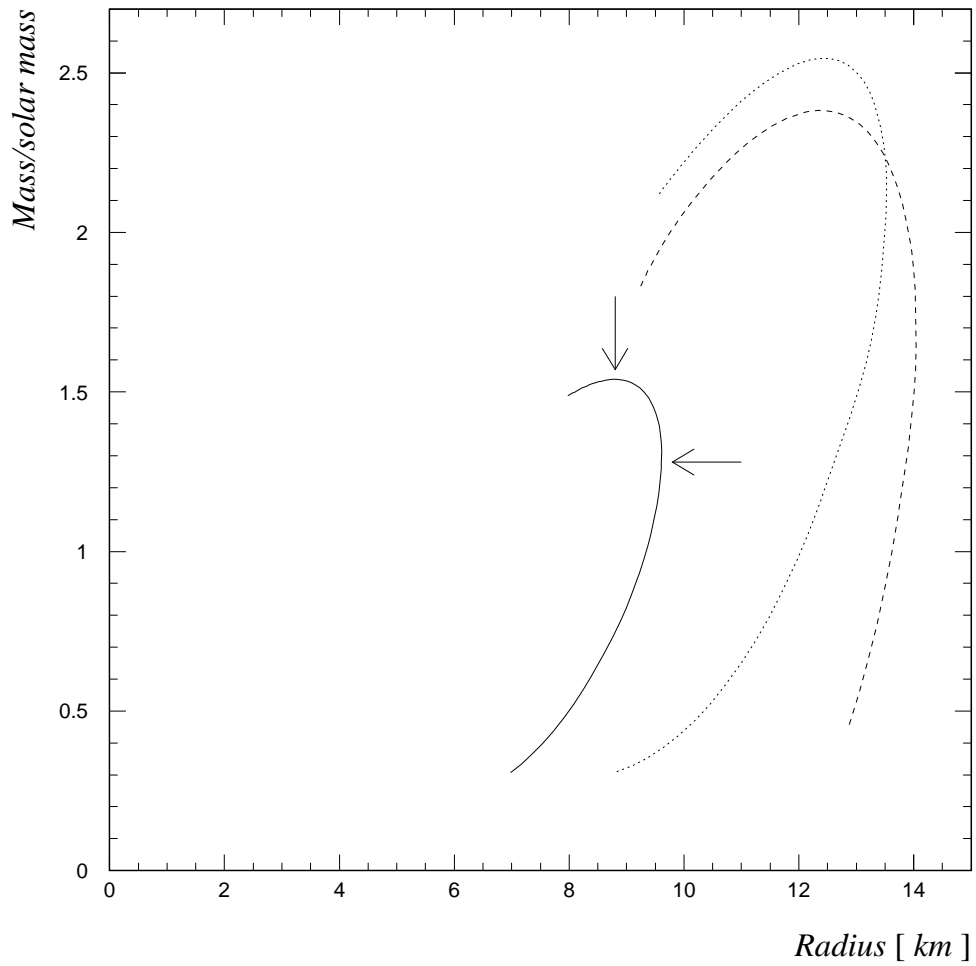


FIG. 4. Total mass M/M_{\odot} as function of R . Notations are the same as in Fig. 3. The arrows indicate the maximum and minimum mass obtained with the CDM EOS.